AT THE ENTERPRISES AND INSTITUTES

UDC 666.762.43:546.422:546.88

SELF-PROPAGATING HIGH-TEMPERATURE SYNTHESIS OF CERIUM CHROMITE SUBSTITUTED WITH ALKALINE-EARTH METALS

M. V. Kuznetsov[1] and Yu. G. Morozov[1]

Translated from Steklo i Keramika, No. 4, pp. 27 – 31, April, 2004.

Cerium chromites, non-substituted and substituted with alkali-earth metals, are synthesized in the self-propagating high-temperature synthesis mode using solid interaction oxidizes. The characteristic temperatures and specifics of interaction between the components are determined for all systems considered. The structural and physicochemical parameters, including the spectroscopic characteristics of the synthesis products depending on the alkaline-earth metal substituent and the degree of substitution, are investigated.

Compounds of rare-earth elements of the type $LnMO_3$ (Ln used for rare-earth metals (REM) and M used for Cr, Mn, Fe) belong to the structural type of perovskite-like oxides analogous of $CaTiO_3$ and have the same crystal structure isostructural to gadolinium ferrite. The intense interest in the synthesis and properties of this class of chemicals is related to their extensive application in contemporary engineering as materials for high-temperature heaters and thermoelectric devices, in the nuclear power industry, and as electrodes for different purposes. Materials of this class also have vast prospects for use as cathode or binding elements in cellular structures. In developing alternative power sources, REM of this type are used in a non-substituted form, or with partial replacement of REM or M in these compounds by an alkaline-earth metal (Mg, Ca, or Sr) with the aim of increasing the chemical resistance of materials in the oxidizing and reducing atmospheres and raising their electric conductivity. Self-propagating high-temperature synthesis (SHS) of such materials without additives or with substitution (applied to Ln – La composites) was carried out earlier [1 – 3]. At the same time, experimental studies of cerium compounds and their properties are very scarce, as their synthesis involves difficulties due to the variable valence of cerium.

The present paper investigates the processes of SHS of non-substituted cerium chromites and cerium chromites with additives of alkaline-earth metals (AEM), as well as various physicochemical characteristics of these materials. Complex cerium oxide compounds are used in different sectors of industry as catalysts, refractories, luminophores, and for other specialized purposes. The use of cerium compounds as materials for industrial electrodes has lately found practical application in the electrolytic production of metals. The possibility of two types of cerium ions (Ce^{4+} and Ce^{3+}) coexisting in the synthesis of such materials intensifies the electrolytic processes and, accordingly, increases the yield of metal per volume unit of electrode consumed. At the same time, the formation of Ce^{4+} cerium ions can be partly compensated by introducing bivalent ions of alkaline-earth metals Ca^{2+} and Sr^{2+} due to the cerium deficit. The synthesis of cerium chromite $CeCrO_3$, non-substituted or with AEM additives, can be performed in special conditions using cerium oxide (or sesquioxide) as a cerium source in the reaction or in normal conditions using cerium dioxide according to the equations

$$(1-x)CeO_2 + xCaO + Cr + yNaClO_4 \rightarrow Ce_{1-x}Ca_xCrO_3 + yNaCl;$$

$$(1-x)CeO_2 + xSrCO_3 + Cr + zNaClO_4 \rightarrow Ce_{1-x}Sr_xCrO_3 + zNaCl + xCO_2\uparrow;$$

$$CeO_2 + xMgO + (1-x)Cr + kNaClO_4 \rightarrow CeCr_{1-x}Mg_xO_3 + kNaCl,$$

where $x = 0 – 0.3$.

In each specific case the quantity of solid intrareaction oxidizer ($NaClO_4$) was calculated expecting complete oxida-

[1] Institute of Structural Macrokinetics and Problems of Science of Materials, Russian Academy of Sciences, Chernogolovka, Moscow Region, Russia.

0361-7610/04/0304-0127

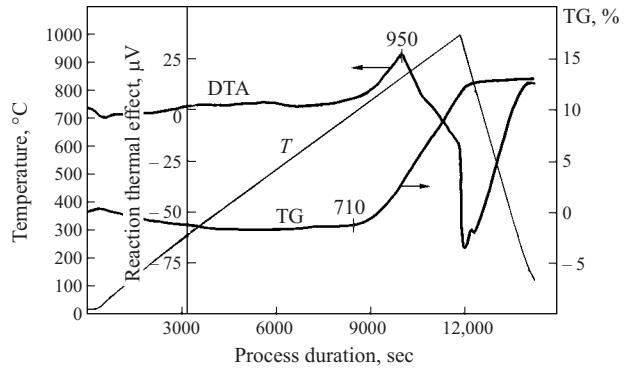

Fig. 1. TG, DTA, and temperature *T* curves of the process of oxidation of metallic chromium powder (PKhM-1) in air under linear heating.

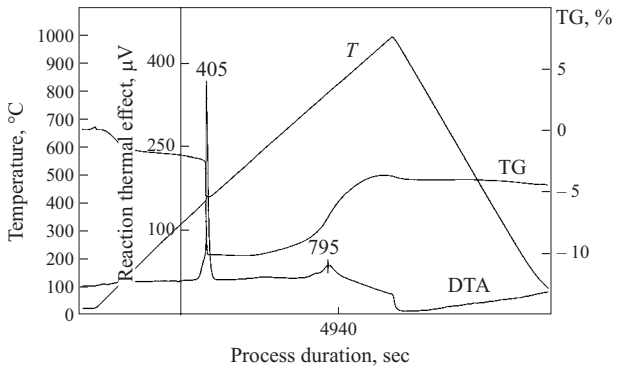

Fig. 2. TG, DTA, and temperature *T* curves of the process of interaction between components of $CeO_2 + Cr + NaClO_4$ mixture under linear heating – cooling.

tion of all metallic chromium in the system to Cr^{3+} (y, z, $k = 0.325 – 0.175$). Ions with a large radius such as Ca^{2+} (0.104 Å) and Sr^{2+} (0.120 Å) in the structure of this material occupy mainly the positions of the REM ($r_{Ce^{4+}} = 0.088$ Å, $r_{Ce^{3+}} = 0.103$ Å), whereas the Mg^{2+} ion, which is significantly smaller in radius (0.074 Å), predominantly occupies the octahedral positions and, accordingly, incorporation of magnesium into the material structure proceeds due to the chromium deficit ($r_{Cr^{3+}} = 0.064$ Å, $r_{Cr^{4+}} = 0.055$ Å).

The infrared spectra were recorded in the reflection mode using a Nicolet 205 instrument (France). The disk-shaped samples (diameter 13 and thickness 1 mm) were molded from the powders synthesized and a thinning agent KBr (sample : thinning agent ratio 1 : 20, sample weight approximately 10 mg). The molding pressure was 600 MPa. The ultraviolet spectra were recorded using a Testscan Shimadzu UV instrument (Japan) for samples prepared in the same way.

Since the solid oxidizers used in SHS are perchlorates of alkali materials (in this case sodium), it is interesting to investigate the process of oxidation of powders of transition metals in the presence of these perchlorates. Several characteristic temperature ranges can be isolated in the process of decomposition of perchlorates. The range of the transition of a stable rhombic β-modification of sodium perchlorate into the cubic α-modification is very wide and accompanied by an endothermic peak in the range of 100 – 360°C. Its partial dehydration takes place within this temperature range. Furthermore, perchlorate melting is accompanied by an endothermic peak with a maximum at 475°C and transforms into the process of its decomposition according to the scheme

$$NaClO_4 \rightarrow NaCl + 2O_2\uparrow.$$

At 590 – 600°C a phase transformation is registered as well in the structure of emerging sodium chloride, and its melting is observed at 801°C.

The experiments (temperatures range 20 – 1200°C, heating/cooling rate 10 K/min) demonstrate that oxidation of metallic chromium powder starts at a temperature of 710°C with maximum heat release at 850°C (Fig. 1). The sample weight increment is 13.3%, which corresponds to partial occurrence of the reaction:

$$2Cr + 1.5O_2 \rightarrow Cr_2O_3.$$

The exothermic process of metallic chromium oxidation that has a catalytic effect on the decomposition of sodium perchlorate proceeds at a temperature 200°C lower than the temperature of metal oxidation in the air atmosphere, i.e., at about 400°C (versus approximately 600°C). This process is due to the emission of active intrareaction oxygen in the decomposition of the solid oxidizer. The reactions in the $NaClO_4 – Cr$ system are highly exothermic; consequently, partial desorption of sodium chloride vapor (according to chemical analysis data, more than 70 wt.%) from the reaction zone is registered at high temperatures (vapor pressure 10 Torr at a temperature of 1014°C).

The studies performed in the linear heating regime (maximum temperature 1000°C, rate of heating/cooling 10 – 20 K/min) established that the maximum heat emission (about 360 μV) in the system $CeO_2 – Cr – 0.25NaClO_4$ related to oxygen desorption from sodium perchlorate occurs at a temperature of 400 – 405°C (Fig. 2). This thermal effect is accompanied by weight losses (about 8%). Prior to that, a weight loss (over 2%) is registered in the sample due to its dehydration at the initial stage of the process (100 – 150°C). Subsequently, a weight increment is registered on the TG curve at about 600°C related to the oxidation of metallic chromium. This process is accompanied by an exothermic peak on the DTA curve with a maximum at 795°C. The substantial time and temperature difference between the processes of oxygen desorption and metal oxidation is leveled in SHS synthesis due to the presence of a substantial temperature gradient in the combustion waves (over 3000 K/sec). At a temperature above 900°C a flat segment appears on the TG

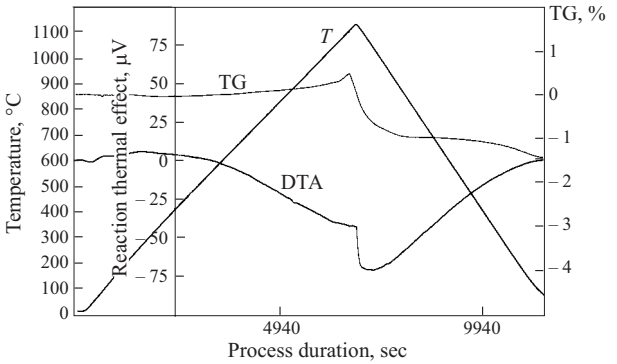

Fig. 3. TG, DTA, and temperature T curves of the process of linear heating – cooling of SHS-synthesized cerium orthochromite $CeCrO_3$ (in $CeO_2 + Cr + NaClO_4$ system); temperature range 20 – 1150 – 20°C.

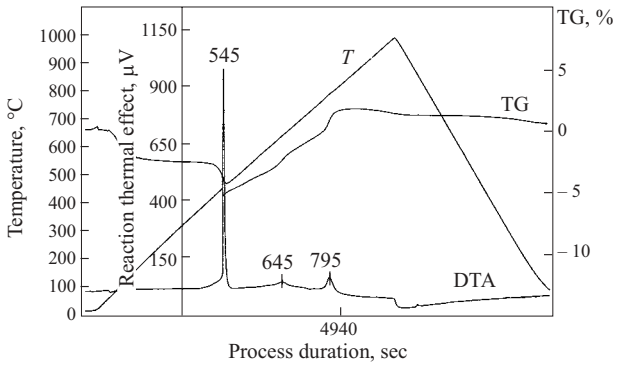

Fig. 4. TG, DTA, and temperature T curves of the process of interaction between components of $CeO_2 + CaO + Cr + NaClO_4$ mixture ($x = 0.3$) under linear heating – cooling.

curve, which is due to the completion of chromite formation and oxidation of metallic chromium. The DTA curve of cerium chromite produced by SHS does not exhibit perceptible thermal effects in the temperature interval of 20 – 1100°C (Fig. 3). A slight increment in the sample weight is registered only at a temperature of 1100 – 1120°C, which is presumably related to the start of partial oxidation of cerium chromite proper according to the reaction

$$2CeCrO_3 + 0.5O_2 \rightarrow 2CeO_2 + Cr_2O_3.$$

This is evidence of a significantly higher thermal resistance and a significantly lower number of defects in SHS products as compared to cerium chromite synthesized according to the standard technology [4, 5].

The introduction of calcium oxide ($x = 0.3$) into the batch due to a deficit of cerium oxide brings the temperature of the maximum heat release caused by oxidation of metallic chromium down to 540 – 545°C (Fig. 4). This suggests that the introduction of this particular oxide has an inhibiting effect on initiation of the process of decomposition of sodium perchlorate. At the same time, heat emission in this system proceeds more intensely (the thermal effect is approximately 950 μV). The emergence of an additional peak with a maximum at 645°C on the DTA curve is presumably related to the formation of an intermediate product in the system, namely calcium chromate, according to the following scheme:

$$2CaO + Cr_2O_3 + 1.5O_2 \rightarrow 2CaCrO_4.$$

Simultaneously with this process, cerium chromite and to a lesser extent cerium chromate in formed in accordance with the reactions

$$2CeO_2 + Cr_2O_3 \rightarrow 2CeCrO_3 + 0.5O_2\uparrow; \quad (1)$$

$$2CeO_2 + Cr_2O_3 + 0.5O_2 \rightarrow 2CeCrO_4. \quad (2)$$

The heat emission maximum (on the DTA curve) in the course of formation of calcium-substituted product of synthesis is registered at the same temperature as in the synthesis of non-substituted material, i.e., 795°C, due to crystallization of the product of synthesis from the solutions in the melt according to the following reactions:

$$(1 - x)CeCrO_3 + xCaCrO_4 \rightarrow Ce_{1-x}Ca_xCrO_3 + 0.5xO_2\uparrow; \quad (3)$$

$$(1 - x)CeCrO_4 + xCaCrO_4 \rightarrow Ce_{1-x}Ca_xCrO_3 + 0.5O_2\uparrow. \quad (4)$$

However, a flat segment and, accordingly, the end of metal oxidation are registered at lower temperatures (850 – 870°C) than in the absence of calcium oxide.

In the presence of strontium carbonate $SrCO_3$ ($x = 0.3$) introduced into the system in the same molar ratio, due to the deficit of CeO_2 the process and its temperature dependences change as well. The maximum heat emission on the DTA curve is registered at 460°C, which is also higher than the temperature of the respective effect in a non-substituted system. However, the inhibiting effect of strontium carbonate is significantly less perceptible than that of calcium oxide. In this system an additional two-stage exothermic effect with maximums at 610 and 650°C is registered on the DTA curve. This is related to simultaneous processes of decomposition of strontium carbonate and formation of strontium chromate according to the schemes

$$SrCO_3 \rightarrow SrO + CO_2\uparrow;$$

$$2SrO + Cr_2O_3 + 1.5O_2 \rightarrow 2SrCrO_4.$$

Further on, the process is analogous to reactions (1) – (4) with crystallization of the substituted product of synthesis from the solution in the melt of strontium chromate and cerium chromite-chromate. The temperature of the maximum heat release on the DTA curve in the formation of the synthesis product and the temperature of formation of the flat segment (which is related to the completion of chromium oxidation) on the TG curve (810 – 820°C) virtually do not differ from the respective temperatures in formation of the calcium-substituted product.

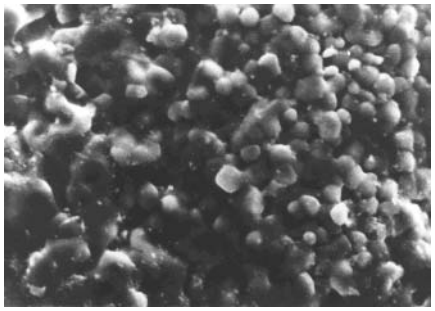

Fig. 5. Microphoto of cerium chromite.

In the synthesis of magnesium-substituted structures the thermal effect maxima on the DTA curve at temperatures of 450 – 460 and 690°C, as well the weight increment effect on the TG curve caused by oxidation of metallic powder at high temperatures (above 700°C), are less clearly expressed due to the deficit of material in the system (0.7Cr).

Tetravalent cerium compounds with AEM oxides of the $A^{2+}B^{4+}O_3$ type is not formed in SHS of cerium chromites substituted with AEM. This is due to the fact that the temperature range of the formation of AEM cerates significantly exceeds the maximum temperatures of SHS processes in this particular system (for instance, the temperature of $CaCeO_3$ formation is 1400°C).

There is yet no unified opinion regarding the parameters of the elementary cells of substituted and non-substituted cerium chromite, nor of its crystallization syngony. It is known that cerium chromite crystallizes in the cubic syngony *Pm*3*m* (221) with the parameter $a = 3.85 – 3.89$ and density $6.84 – 6.92$ g/cm^3. However, later publications attribute it to the orthorhombic syngony *Pbnm* with the parameters $a = 5.475$ Å, $b = 5.475$ Å, $c = 7.740$ Å or $a = 6.1$ Å, $b = 8.1$ Å, $c = 5.6$ Å [6, 7]. Non-substituted cerium chromite, which is a product of SHS, crystallizes in the orthorhombic syngony and is isostructural to gadolinium ferrite. The unit cell parameters of $CeCrO_3$ as a SHS product are: $a = 5.495$ Å, $b = 5.486$ Å, $c = 7.717$ Å, $V = 232.63$ Å^3, angle between planes [110] and $[\bar{1}10]$ 89°54′. Unfortunately, the authors have not found any data in the literature on the unit cell parameters of substituted cerium chromites. The calculation of these parameters in SHS products performed using the Comphys and Unit Cell software packages made it possible to follow the dynamics of their variation depending on x and the substituent AEM. Although the ionic radii of calcium and strontium are larger than the ionic radius of cerium, there is an insignificant increase in the pseudocubic parameter a in these systems with increasing x. This agrees with the data in [2, 3] on the variations in the lattice constant in AEM-substituted lanthanum chromites. Obviously, substitution of cerium with larger-radius ions (Ca and Sr) by itself cannot decrease the lattice constant. Apparently, in this case part of the charge of the chromium cations change at the same time, which is related to the formation of an electroneutral structure. Part of the chromium Cr^{3+} cations oxidize to Cr^{4+} with a smaller ionic radius ($r_{Cr^{3+}} = 0.064$ Å, $r_{Cr^{4+}} = 0.055$ Å), for instance, according to the scheme $Ce_{1-x}Sr_xCr^{3+}_{1-x}Cr^{4+}_xO_3$.

This structural rearrangement has a perceptibly greater effect on the unit cell volume of the SHS product than replacement of cerium by AEM in the REM positions. This leads to a general decrease in the unit cell volume with increasing x. The same fact accounts for the effect of a increasing with increasing x in the magnesium-substituted system. The partial substitution of magnesium (an ion with a larger radius: $r_{Mg^{2+}} = 0.074$ Å) for chromium leads to an increase in a with increasing x and is not compensated by a possible rearrangement of the total ion charge in the cerium sublattice ($Ce^{3+} – Ce^{4+}$).

TABLE 1

Compounds	a, Å	d, g/cm^3	ρ, m^2/g	χ, Gs · cm^3/g*
$CeCrO_3$	3.878	6.7	0.9	0.111
$Ce_{0.9}Ca_{0.1}CrO_3$**	3.876	6.4	0.3	0.110
$Ce_{0.8}Ca_{0.2}CrO_3$	3.873	6.2	0.4	0.109
$Ce_{0.7}Ca_{0.3}CrO_3$	3.870	5.8	0.5	0.108
$Ce_{0.9}Sr_{0.1}CrO_3$	3.877	6.5	2.2	0.076
$Ce_{0.8}Sr_{0.2}CrO_3$	3.875	6.2	2.4	0.063
$Ce_{0.7}Sr_{0.3}CrO_3$	3.872	5.7	4.3	0.060
$CeCr_{0.9}Mg_{0.1}O_3$	3.879	6.3	1.4	0.076
$CeCr_{0.8}Mg_{0.2}O_3$	3.880	6.1	1.8	0.042
$CeCr_{0.7}Mg_{0.3}O_3$	3.882	5.5	2.9	0.035

* Magnetic field intensity 10 kOe.

** Ca and Mg additives were introduced via CaO and MgO, and Sr additive was introduced via $SrCO_3$.

The specific surface areas ρ of non-substituted REM chromite powders produced by SHS (including cerium chromite) are within the limits of 0.3 – 1.0 m^2/g, which points to the formation of rather coarse powder fractions in combustion (Table 1). According to the electron microscopy data, the mean particle size of the nonsubstituted product $CeCrO_3$ is 1 – 5 μm (Fig. 5) As x grows from 0.1 to 0.3, the specific surface areas of substituted cerium chromite powders increase for each AEM. The absolute values of the pycnometric densities of the respective SHS-produced chromites are lower than those of chromites synthesized by other methods. This may be related to the substantial gas emission from samples in combustion and, accordingly, to the increased porosity and microporosity of the products.

The magnetic properties of cerium chromites are classified as weak antiferromagnetics with the Dzialosinski effect, i.e., antiferromagnetics with a weak spontaneous magnetic moment. One important magnetic parameter is the magnetic susceptibility χ. The values of χ in weak ferromagnetics are significantly lower than in strong ones. Measurements per-

formed at a temperature of – 190°C (83 K) in a magnetic field of intensity 10 kOe indicated that this parameter in SHS-produced cerium chromites is within the limits of $0.111 – 0.035\ G \cdot cm^3/g$ depending on the substituent element, the value of x, and the AEM.

It can be see in Table 1 that with increasing x the pycnometric density d of the products of synthesis and specific magnetic susceptibility χ decrease. The latter effect is presumably a result of weakening of exchange interaction between the chromium atoms when an AEM is substituted for cerium in the crystal structure of cerium chromite. This effect is more perceptible in the substitution of AEM for chromium with a magnesium additive introduced. The resistivity, on the contrary, grows with increasing x and, for instance, in calcium-substituted samples increases from $30\ \Omega \cdot cm$ at $x = 0.2$ to $1000\ \Omega \cdot cm$ at $x = 0.3$. Analysis performed using Raman spectroscopy (resolution 1 μm) indicate that adding strontium into cerium chromite even in small concentrations ($x = 0.1$) leads to the formation of an additional band at 840 cm^{-1} related to the formation of the Sr – O bonds in the structure, in addition to the absorption bands of the non-substituted material (Fig. 6). The TCLE of materials without additives grows with increasing x. In strontium- and calcium-substituted systems with x growing to 0.3 the TCLE grows by nearly 20%. The absorption share grows as well in the UV spectrum of strontium-substituted cerium chromite. At the same time, the general configuration of the spectra of strontium-substituted samples changes compared to the samples with $x = 0$. An additional absorption peak appears in the substituted samples in the range of 320 – 330 nm, which is typical, since its structure contains an AEM.

The IR spectra of substituted samples exhibit a shift in the structure of Cr – O bonds toward lower frequencies and decreased vibrations of the O – Cr – O bonds. Within the range of 1000 – 400 cm^{-1} there are two main absorption bands (590 and 420 cm^{-1}) in the structure of nonsubstituted $CeCrO_3$. The position of these bands does not change even with high concentrations of Ca and Sr. Furthermore, the spectra of the strontium-substituted sample has two additional absorption bands (890 and 850 cm^{-1}) typical of the spectrum of strontium chromate, which is evidence of the incorporation of the AEM into the structure of the product of synthesis. In the case of substituting calcium for cerium ($x > 0.1$), cerium chromite as well exhibits two additional absorption bands in the range above 850 cm^{-1}, along with two main characteristic bands. However, their intensity is significantly lower than that of the respective bands in the strontium-substituted samples, which is evidence of an increasing effect of the substituent AEM on the IR spectra of chromite, as the atomic number of the AEM increases.

The modification of the spectrum of the magnesium-substituted product differs from the spectra of materials containing AEM described above, since substitution in this material occurs in the positions of chromium and not cerium. The

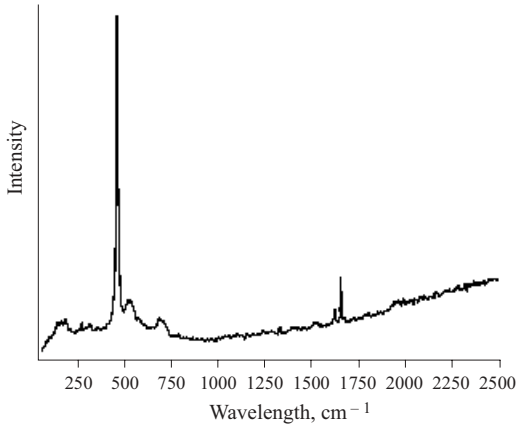

Fig. 6. Raman spectrum of cerium chromite (SHS product) in the range of 50 – 2500 cm^{-1}.

Cr – O bonds are significantly more sensitive to the formation of defects directly in their structure than to the presence of defects in the REM sublattice. Thus, even with low concentrations of magnesium ($x = 0.1$) the intensity of the band at 420 cm^{-1} perceptibly decreases and the band at 590 cm^{-1} is split into two bands with maxima at 585 and 630 cm^{-1}. As the degree of substitution of magnesium for chromium grows ($x > 0.1$), the intensity of the band at 420 cm^{-1} becomes negligibly low and its maximum cannot be identified. At $x = 0.2$ or greater, only one maximum is registered at 630 cm^{-1} in the material spectrum within the range of 1000 – 400 cm^{-1}, which is due to significant weakening of the Cr – O bonds and strengthening of the Mg – O bonds.

Thus, cerium chromites, non-substituted and substituted with alkaline-earth metals, have been synthesized in combustion in an air medium using only solid intrareaction oxidizers. The SHS products have higher thermal resistance and fewer structural defects compared to products obtained according to the standard ceramic technology. As a consequence of model experiments in the heating-cooling regime, the characteristic temperatures of oxidation, decomposition of initial reactants, and formation of the products of synthesis were determined. The processes of formation of SHS products with AEM additives proceed with the formation of intermediate chromates of the respective AEM.

The SHS process generates coarse powder fractions of complex oxides with lower specific surface areas and pycnometric densities than in the products of coprecipitation of reactants and synthesis under firing in the furnace. With growing x the elementary cell parameters change and the magnetic susceptibility of chromites decreases due to weakening of exchange interaction between the chromium atoms. The Raman UV and IR spectra of chromites exhibit additional absorption bands, which is caused by incorporation of AEM into the structure of the products of synthesis, weakening of Cr – O bonds, and simultaneous formation and intensification of AEM – O bonds.

The study has been performed with financial assistance of the Fund for Assisting Domestic Science, The Royal Society (UK), and a grant from the President of the RF within the program "Young Doctors of Sciences" (MD-216.2003.03).

REFERENCES

1. M. V. Kuznetsov, "SHS of chromites of rare-earth metals," *Neorg. Mater.*, **34**(10), 1264 – 1267 (1998).
2. M. V. Kuznetsov, S. G. Bakhtamov, Yu. G. Morozov, et al., "SHS of strontium doped lanthanum chromites," *Mendeleev Comm.*, No. 4, 136 – 138 (2000).
3. M. V. Kuznetsov, S. G. Bakhtamov, and Yu. G. Morozov, "Self-propagating high-temperature synthesis of strontium-doped lanthanum chromite," *Izv. Vuzov, Ser. Khim. Khim. Tekhnol.*, **43**(4), 46 – 49 (2000).
4. A. I. Leonov, A. B. Andreeva, V. E. Shvaiko-Shvaikovskii, and É. K. Keller, "High-temperature chemistry of cerium in cerium oxides – Al_2O_3, Cr_2O_3, Ga_2O_3 systems," *Neorg. Mater.*, **2**(3), 517 – 523 (1966).
5. V. E. Shvaiko-Shvaikovskii, B. F. Yudin, and A. I. Leonov, "Thermodynamic properties of cerium chromite," *Neorg. Mater.*, **4**(6), 925 – 930 (1968).
6. N. Patibandla, T. A. Ramanarayanan, and F. Cosandey, "Effect of ion-implanted cerium on the growth rate of chromia scales on Ni – Cr alloys," *J. Electrochem. Soc.*, **138**(7), 2176 – 2184 (1991).
7. *Chemical Encyclopedia. Vol. 5* [in Russian], SÉ, Moscow (1988 – 1996).